CrystEngComm

Accepted Manuscript

ROYAL SOCIETY OF CHEMISTRY

www.rsc.org/crystengcomm

Cite this: DOI: 10.1039/c0xx00000x

www.rsc.org/xxxxxx

ARTICLE TYPE

A single precursor approach for ZIFs synthesis: Transformation of a new 1D [Zn(Im)(HIm)$_2$(OAc)] structure to 3D Zn(Im)$_2$ frameworks

Qi Shi,[a] Fei Wang,[a] Xiaozhen Kang,[a] Jun Xu,[b] Yining Huang,*[b] Jinping Li[a] and Jinxiang Dong*[a]

Received (in XXX, XXX) XthXXXXXXXXX 20XX, Accepted Xth XXXXXXXXX 20XX

DOI: 10.1039/b000000x

The solvent free reaction of Zn(OAc)$_2$ with an imidazole ligand resulted in a 1-dimensional (1D) chain structure with a formula, [Zn(Im)(HIm)$_2$(OAc)] (Im =imidazolate, HIm = imidazole, OAc=carboxylate) (1). The results by kinetic experiments suggest that (1) likely evolves from an unidentified metastable phase. This new 1D chain precursor (1) is a quaternary system comprising of Zn, Im, OAc and HIm. We have used this 1D compound as a single precursor to prepare 3-dimensional (3D) Zn(Im)$_2$ frameworks. Specifically, two Zn(Im)$_2$ frameworks with known zni and coi topologies were prepared via thermal-mediated transformation when heated in open atmosphere and in a closed vessel, respctively. In open atmosphere, the kinetic experiments confirmed the rapid phase transformation from (1) to zni without formation of an intermediate phase. In contrast, in the formation process of coi in a closed vessel, phase transformation from (1) to zni and immediately from zni to coi was observed, respectively. Thus, in a closed vessel, the released molecules, HOAc and HIm, were occluded in the framework, which may together exert a cooperative structure-directing effect on the formation of coi framework. Thus, a single precursor approach was established for the synthesis of ZIFs. The present work represents the first example of transforming a 1D coordination polymer into 3D ZIF framework structures.

1. Introduction

Zeolitic imidazolate frameworks (ZIFs) are a subclass of metal-organic frameworks (MOFs), which consist of tetrahedral units of MN$_4$ (M=Co, Zn, etc.) linked by imidazolate ligands.[1] ZIFs often possess expanded zeolite topologies due to the similarity between the coordination angle of the imidazole ligand (N-M-N) and the Si–O–Si angle.[1] Many ZIFs posses the structures and the properties of zeolites as well as those of MOFs or the combination of the two.[2-7] Comparing with MOFs and zeolites, the field of ZIF synthesis is still relatively young. Research in ZIF synthesis is to establish a variety of synthesis concepts, methodologies and strategies as different methods and strategies can lead to new compounds with novel topologies or known compounds with different morphologies.[2-8] From a practical viewpoint, it is also important to establish facile, inexpensive and scaled-up synthesis routes.[3b,9] Furthermore, optimization of these procedures as well as a mechanistic understanding of the crystallization processes also requires the application of different synthesis approaches and strategies.[10]

For ZIF synthesis, the synthesis methods and strategies employed in MOF and zeolite synthesis have also been adopted by different research groups. Initially, several research groups systematically explored the rich structural diversity of ZIFs by using a solvothermal method and ligand-directed strategy.[2-7] Later, several synthesis approaches have also been used for ZIF synthesis including microwave[11], ionothermal synthesis[12], mechanochemistry[13], ultrasonic[9,14], steam-assisted conversion[15], room temperature synthesis[16], accelerated aging[17] and solvent-assisted linker exchange[18]. Normally these synthesis routes are typically based on the reaction between a selected metal salt and the ligand. The starting materials generally employed are imidazole and/or its derivatives and a metal salt in the form of its nitrate, acetate, hydroxide and/or metal oxide.

A single precursor approach that has previously been explored for construction of molecular sieves. The chain aluminophosphate was used as aluminium and phosphorous single-source in the synthesis of SAPOs and AlPOs molecular sieves[19]. Similar transformation was also reported in MOFs[20]. Thus, we speculated whether a similar result could be accomplished in ZIF synthesis.

Our original goal was to attempt a solvent-free synthesis of ZIFs. The solvent-free reaction of Zn(OAc)$_2$ with an imidazole ligand resulted in a 1-dimension (1D) chain structure with the formula Zn(Im)(HIm)$_2$(OAc) (Im=imidazolate, HIm=imidazole, OAc=carboxylate). The new 1D chain precursor was a quaternary system comprising of Zn, Im, OAc, and HIm, which inspired us to propose and devise a single precursor approach to prepare 3-dimensional (3D) Zn(Im)$_2$ framework. Additionally, conversion from the Zn(Im)(HIm)$_2$(OAc) structure to the Zn(Im)$_2$ framework undergoes a 1D–3D transformation. To date, only a few examples involving 2D/3D–3D transformations of ZIFs have been reported[21, 22], none of which involves transformation from a 1D chain structure to a 3D ZIF. Additionally, more experimental study of structural transformations of simple source or precursor to ZIF framework will be helpful in understanding the formation

mechanism of ZIF materials, which is important to rationally develop materials with tailored structural, compositional, and morphological properties.

2. Experimental section

2.1 Materials

The reagents used in the experiments were zinc acetate [$Zn(OAc)_2$, 99.0 wt%, Aladdin Reagent Chemical Co.], imidazole [HIm, 98.0 wt%, Sigma–Aldrich Chemical Co.], N,N-Dimethylformamide [DMF, 99.5 wt%, Tianjin NO.3 Chemical Reagent Factory], Ethanol [CH_3CH_2OH, 99.7 wt%, Tianjin NO.3 Chemical Reagent Factory] and Methanol [CH_3OH, 99.5 wt%, Tianjin NO.3 Chemical Reagent Factory].

2.2 Synthesis and transformation

Synthesis of [Zn(Im)(HIm)$_2$(OAc)] (1)

Synthesis of (1): $Zn(OAc)_2$ (0.184 g) and imidazole (0.408 g) were mixed after grinding in a 120 mL Teflon-lined stainless steel autoclave at 100 °C for 24 hours. After cooling to room temperature, the solid products were separated by filtration and washed with ethanol (50 mL) three times. A large amount of block-like crystals were obtained with a yield of 49.1 % (based on zinc salt). Good quality crystals suitable for single crystal X-ray diffraction were also obtained (CCDC 1044169). Elemental analysis calcd (%) for (1): C 40.3, H 4.27, N 25.6; found: C 40.0, H 4.32, N 24.6. The crystallization process of (1) were performed as a function of reaction time at 100 °C.

Transformation induced by thermal treatment

zni (2): 0.2 g of (1) was carefully placed over an open alumina boat, heated in air at a heating rate of 5 °C min^{-1} to a set temperature (100–450 °C) and maintained at this temperature for 24 h. Afterward, the products were transferred to a desiccator and cooled to room temperature. The typical example zni (2) was obtained at 350 °C. The polycrystalline aggregates were obtained with a yield of 83.8 % (based on zinc). The transformation of (1) to zni (2) in open atmosphere were performed as a function of temperature which was increased at a rate of 5 °C min^{-1}.

coi (3): 0.2 g of (1) was sealed in a 30 mL Teflon-lined stainless steel autoclave, heated at a heating rate of 5 °C min^{-1} to a set temperature (100–220 °C) and maintained at this temperature for 24 h. After cooling to room temperature, the solid products were separated by filtration and washed with ethanol (10 mL) three times.. The typical example coi (3) was obtained at 180 °C. A large amount of small polyhedral crystals were obtained with a yield of 41.3 % (based on zinc). The transformation of (1) to coi (3) in a closed vessel were performed as a function of reaction time at 150 °C.

2.3 Measurements

PXRD patterns were recorded on an X-ray diffractometer (MiniFlex Ⅱ, Rigaku) using Cu Kα radiation (λ = 1.5418 Å). TG-DSC measurements were performed under an air atmosphere on a simultaneous thermal analyzer (Setaram, Labsys evo) at a heating rate of 5 °C min^{-1}. IR spectra were measured using KBr pellets on an FT-IR spectrometer (IRAffinity-1, SHIMADU). CHN analysis was carried out on an elemental analyzer (Elementar, Vario EL III). Zn contents were determined by using an atomic absorption spectrophotometer (Thermo Fisher Scientific, Solaar S2). SEM micrographs were obtained with a scanning electron microscope (Hitachi, TM3000). Single crystal measurements were carried out on a BrukerSmart-l000 CCD diffractometer with graphite monochromated Mo Ka, (λ=0.071073 nm) radiation.

$^1H \rightarrow {}^{13}C$ cross-polarization (CP) magic angle spinning (MAS) NMR spectroscopy was performed on a Bruker Avance III 600 WB spectrometer at 151 MHz at a magnetic field of 14.2 T using a 4 mm double-tuned MAS probe with a spinning speed of 9 kHz. The Hartmann-Hahn matching conditions were calibrated on solid adamantane, which is also a secondary reference for the ^{13}C chemical shifts (δ_{iso} = 38.48 ppm for the methylene signal). 1H 90° pulse width was 3.1 μs and the pulse delay was 10 s. The contact time was 2 ms.

3. Results and discussion

3.1 Crystalline precursor: 1D chain structure [Zn(Im)(HIm)$_2$(OAc)] (1)

We first carried out a solvent-free synthesis of ZIF due to the low melting point of HIm (88–91 °C) since solvent-free synthesis may lead to effective and environmentally benign routes to ZIF preparation. However, instead of 3D ZIFs, only a 1D chain structure with the formula, [Zn(Im)(HIm)$_2$(OAc)] (1) was formed upon reaction of $Zn(OAc)_2$ with an excess of HIm. Actually, the product is a mixture of (1) and an unidentified phase upon heating $Zn(OAc)_2$ and HIm at 50 °C with initial molar ratios of 1:2 and 1:6 (below the melting point of HIm) (Figure S1, left). And (1) was obtained at 100 °C when the molar ratio of $Zn(OAc)_2$ and HIm is 1:6 and good quality crystals suitable for single crystal X-ray diffraction were obtained. When a $Zn(OAc)_2$/Him ratio of 1:2 was used, an as yet unidentified phase was obtained based on the PXRD result (Figure S1, right). The structure of the unidentified material has not yet been resolved. The bulk purity of (1) was confirmed by comparing its experimental PXRD pattern to that calculated based on the single crystal structure data (Figure S2).

The crystal structure of (1) was determined using single crystal X-ray diffraction (Table S1). (1) crystallizes in the space group $P2_1/c$ and belongs to monoclinic crystal system. It exhibits a 1D chain structure (Figure 1). As shown in Figure 1(a), the asymmetric unit consists of one Zn(II) atom, one deprotonated imidazolate ligand, two imidazole molecules, as well as one free acetate anion. Zn1 adopts a four-coordinated tetrahedral geometry with two nitrogen atoms (N1 and N2) from the deprotonated imidazolate anions and two nitrogen atoms (N3 and N5) from the imidazole molecules. The Zn–N bond lengths lie in the normal range of 1.971(4)–2.005(4) Å and the angle N-Zn-N found for this compound is 104.9°–117.0°. All these bond distances and angles fall in the normal range of those reported for other zinc imidazolate structures in the literature.[2,4] The deprotonated imidazolate anions connect adjacent Zn atoms to form one-dimensional zigzag chains along the b-axis with a Zn1•••Zn1 bond distance of 6.0214(8) Å (Figure 1b).

Cite this: DOI: 10.1039/coxx00000x

www.rsc.org/xxxxxx

ARTICLE TYPE

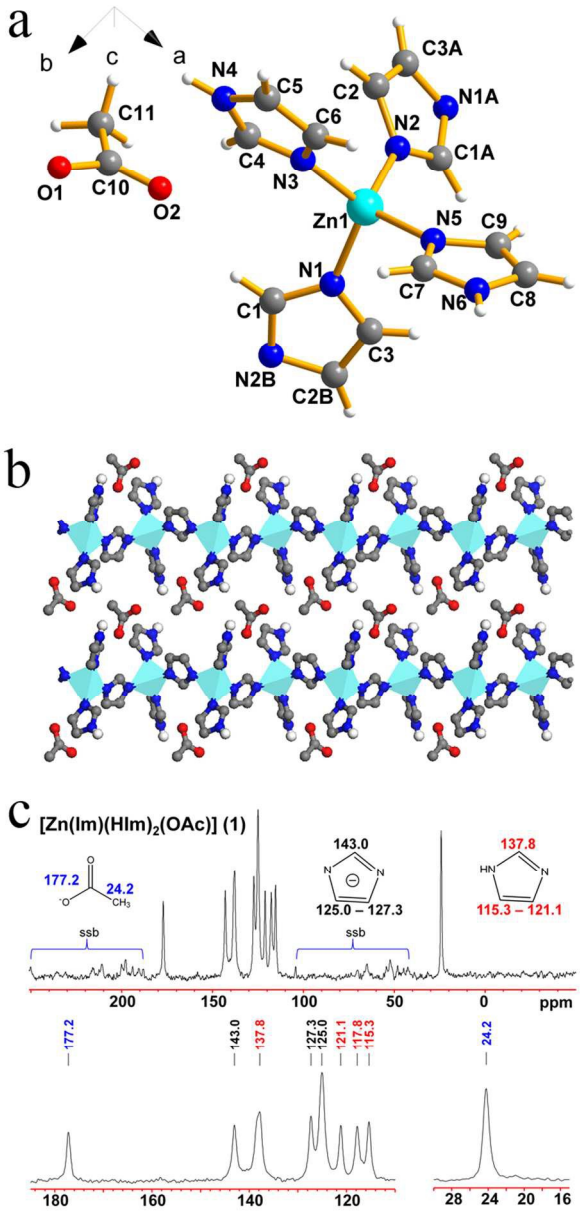

Figure 1 (a) A ball-and-stick representation of the asymmetric unit of $[Zn(Im)(HIm)_2(OAc)]$ (1); (b) a polyhedron representation of (1) viewed parallel to the crystallographic b-axis showing the zigzag Zn-Im-Zn (the hydrogen atoms except hydrogen of NH in HIm were omitted for clarity); and (c) $^{13}C\{^1H\}$ MAS solid-state NMR spectrum of (1) (ssb are the spinning side bands).

Next, ^{13}C solid-state NMR spectroscopy was used as a local probe to elucidate the composition and bonding motifs in (1) (Figure 1c). The presence of both Im and HIm was again confirmed as the signals belonging to Im and HIm are both visible in the spectrum of (1). The resonances at δ = 143.0 and 125.0/127.3 ppm correspond to the carbon atoms in the Im ring. The proton-bearing HIm has signals at δ = 137.8 and 115.3/117.8/121.1 ppm, respectively. The signals pertaining to HIm are shielded with respect to Im. The two additional peaks at δ = 177.2 and 24.2 ppm can be assigned to the carboxyl and methyl carbons in OAc. The spectrum of (1) is in good accordance with the literature-known ^{13}C resonances of the analogous Zn(BeIM)OAc.[23] Thus, the ^{13}C solid-state NMR spectrum is consistent with the single crystal structure. IR spectrum is also in agreement with the above findings (Figure S3). The broad characteristic ν(NH)- stretching vibrations seen in the region between 3300 and 2500 cm^{-1} confirm the presence of HIm in (1). Furthermore, the strong absorbance at 1608 cm^{-1} is due to ν(C=O)-stretching, indicating OAc in (1).

The TG-DSC measurement of (1) was carried out in an air atmosphere from ambient temperature to 1000 °C (Figure S4). The TG trace shows a two-step mass loss in the temperature range 100–300°C. It is noticeable that the mass loss in the TG experiment is about 38.7 wt%, which closely matches one HIm and OAc molecule calculated from the formula $[Zn(Im)(HIm)_2(OAc)]$ (38.8 wt%). However, this does not correspond to the two steps of mass loss of two independent OAc and HIm molecules. Therefore, the mass loss of (1) below 300°C likely indicates the formation of networks with the formula $Zn(Im)_2$. This is corroborated by the PXRD patterns recorded for (1) heated in air (see below: thermal-mediated transformation). The weight loss occurring in the temperature range of 450–650 °C seems due to framework decomposition. The final decomposition product was identified as ZnO by PXRD pattern. This ZnO accounts for approximately 24.8 wt% of the total sample weight, in good agreement with the formation of ZnO, which is calculated at 25.1 wt%.

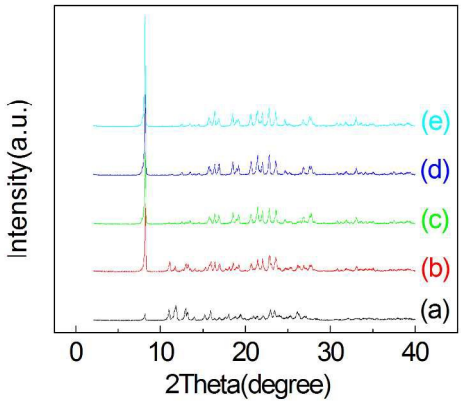

Figure 2 PXRD patterns illustrating the crystallization process of $[Zn(Im)(Him)_2OAc]$ (1) at 100 °C (heated to the reaction temperatures at a rate of 5 °C min^{-1}) as a function of reaction time: (a) 1 h; (b) 3 h; (c) 6 h; (d) 12 h; (e) 24 h.

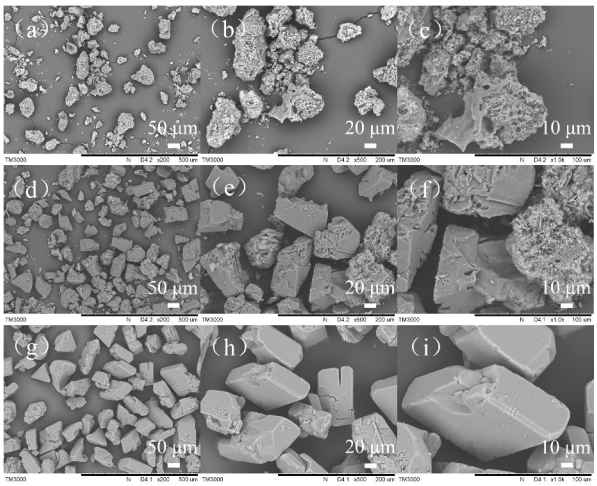

Figure 3 Different magnification SEM images illustrating the crystallization process of $[Zn(Im)(Him)_2OAc]$ (1) at 100 °C (heated to the reaction temperatures at a rate of 5 °C min^{-1}) as a function of reaction time: (a, b, c) 1 h; (d, e, f) 3 h; (g, h, i) 12 h.

To understand the crystallization process in the synthesis of (1), the PXRD patterns of the products obtained after different reaction times are shown in Figure 2. For this particular study, (1) was prepared by heating of the mixture of $Zn(OAc)_2$ and HIm with the molar ratio of 1:6 at 100 °C. After 1 h, a mixture of unidentified phase and small (1) was obtained. In fact, the unidentified phase was also obtained when a $Zn(OAc)_2$/HIm ratio of 1:2 at 100 °C for 24 h (Figure S1, right). The result suggests that (1) likely evolves from this unidentified phase. So, it is important to add HIm in excess to the zinc source. When the reaction time was extended beyond 1 h, the characteristic PXRD peaks of unidentified phase start disappearing and the relative peak intensity of the (1) phase increases, implying reorganization between the unidentified phase and excess Im has occurred. Complete phase transformation was observed after 12 h.

In addition, the formation process of (1) was confirmed by SEM images, as shown in Figure 3 and Figure S5. The metastable phase was observed in SEM images taken after 1 h which show besides the minor fraction of block-like crystals (1) (Figure 3a and Figure S5a), the large number of particles with a irregular aggregate morphology (Figure 3a, b, c) which can be assigned to unidentified phase. After 3 h some block-like crystals of (1) are seen besides unidentified phase in SEM images indicate a mixture of (1) and unidentified phase (Figure 3d, e, f). In SEM images after 12 h the crystals of (1) can be clearly identified by their distinct block-like shape (Figure 3g, h, i). Based on SEM results, most block-like particles have size in range of 100–200 μm. After 12 h good quality crystals suitable for single crystal X-ray diffraction were obtained.

The TG analysis suggests an interesting phenomenon that heating (1) can transform 1D chain structure to a $Zn(Im)_2$ framework. Since the new 1D chain precursor of (1) is a quaternary system comprising of Zn, Im, OAc and HIm, we decided to use the new chain compound of (1) as a single precursor to prepare $Zn(Im)_2$ framework.

3.2 Transformation induced by thermal treatment

Herein, we report the structural transformation of a single precursor, $[Zn(Im)(HIm)_2(OAc)]$ (1) to a $Zn(Im)_2$ framework via thermal treatment (Scheme 1).

We first carried out the thermal mediated transformation from a novel 1D $[Zn(Im)(HIm)_2(OAc)]$ structure (1) to 3D $Zn(Im)_2$ framework in open atmosphere. The identity of the heating products at a set temperature (100–450 °C) was checked using PXRD (Figure S6, left).

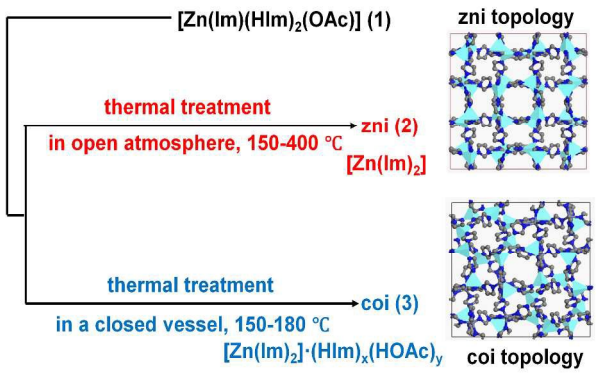

Scheme 1. A schematic diagram for thermal-mediated transformations from 1D chain $[Zn(Im)(HIm)_2(OAc)]$ (1) to 3D $Zn(Im)_2$ framework.

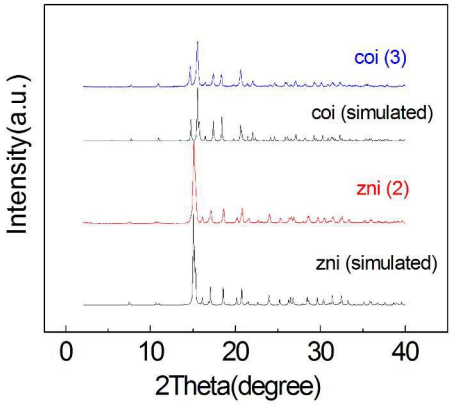

Figure 4. Experimental XRD patterns for the samples (obtained by thermal-mediated transformations) and the XRD patterns simulated from the crystal structure data.

As can be noted, the PXRD studies confirm that (1) is stable up to 100 °C. When heated at 150 °C, all Bragg reflections of (1) disappear and the formation of a $Zn(Im)_2$ framework with zni topology (denoted as zni (2)) is complete, suggesting a structural transformation and reorganization of (1) after removal of the one HIm and OAc molecule (Figure S6). zni is a 3D network of $Zn(Im)_2$, which was reported by Lehnert and co-workers.[24] Heating (1) in the open alumina boat resulting in the formation of zni (2) is accompanied by the release of one HIm and a OAc molecule into the environment. Losing HIm and OAc species means that they can no longer play roles in forming ZIFs. To examine if HIm and OAc have influence on reaction product, we treated (1) using the same procedure, but the compound (1) was heated in a sealed Teflon-lined stainless steel autoclave (Figure

Cite this: DOI: 10.1039/coxx00000x

www.rsc.org/xxxxxx

ARTICLE TYPE

S7, left).

Most strikingly, heating the sample (1) in a closed vessel rather than in open atmosphere leads to the formation of coi topology (denoted as coi (3)) instead of zni topology. coi is a 3D network of $Co(Im)_2$, which was structurally characterized by Sturm et al.[24] coi with $Zn(Im)_2$ was reported by Tian et al. when it was synthesized in solvothermal reactions.[2a] As described beforehand, we observed that (1) was thermally stable up to 100 °C. The PXRD data show that on heating at 150°C, (1) was transformed into a pure phase coi (3). Here, the important finding is that the released HIm molecule and OAc are retained in the closed system, which, in turn, play a crucial role for the formation of coi topology during the structural transformation. This indicates that the product obtained in closed system contains more HOAc or HIm than the product obtained in open system. The purity of the as-synthesized compound zni (2) and coi (3) was confirmed by the similarities between the simulated and experimental PXRD patterns (Figure 4).

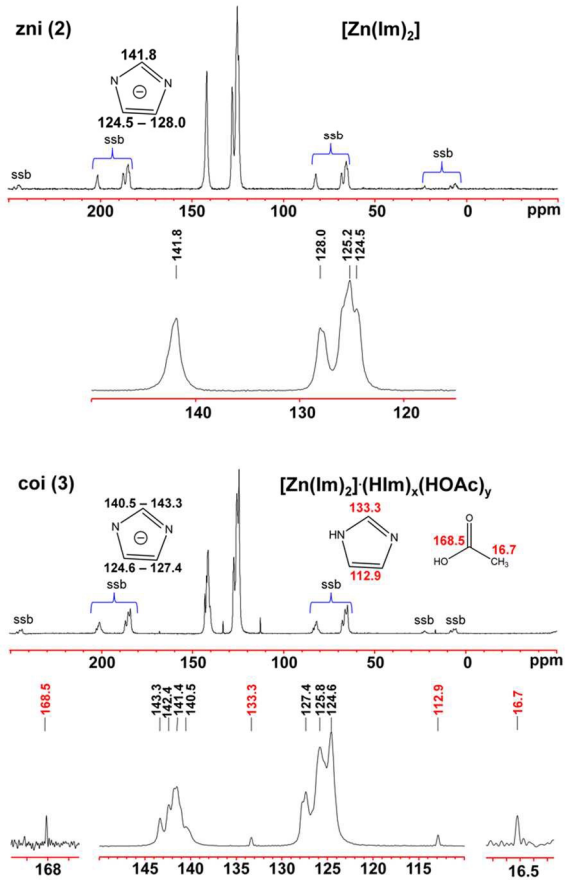

Figure 5. $^{13}C\{^1H\}$ MAS solid-state NMR spectra of the obtained zni (2) (in open atmosphere) and coi (3) (in a closed vessel) via a thermal-mediated transformation (ssb are the spinning side bands).

The above scenario was also confirmed by the ^{13}C solid-state NMR spectra (Figure 5) recorded for zni (2) and coi (3), the same peaks at δ = 124-128 and 140-143 ppm were observed in the spectra of both zni (2) and coi (3) and they originate from the deprotonated bipodal imidazolate ligands in $Zn(Im)_2$. However, in the spectrum of coi (3), two additional groups of signals, one pertaining to the carboxyl and methyl carbons of HOAc (δ = 168.5 and 16.7 ppm) and the other to HIm (δ = 133.3 and 112.9 ppm) were also observed. It appears that in the transformation process from (1) to coi (3)-$[Zn(Im)_2]\cdot(HIm)_x(HOAc)_y$, the released HOAc or HIm molecules were occluded into the framework of coi (3), suggesting that they may together exert a cooperative structure-directing effect on the structural transition from (1) to the coi frameworks. This work provides the first example of HOAc or HIm possibly having a structure-directing effect on the synthesis of a ZIF material.

In the TG analyses performed in air for zni (2), no noticeable mass loss was observed at the temperatures up to 450 °C, at which decomposition of the framework structure commenced (Figure S6, right). In Figure S7 (right) it shows a small ca. 2.7 wt% weight loss for coi (3) occurring at 200–400 °C, which was assigned to the loss of the HOAc or HIm molecules. Analyses of these phase transition samples by solid-state ^{13}C NMR, and TG have provided insight into the origin of the phase transition behavior.

In order to gain a better understanding of the transformation mechanisms of (1) to $Zn(Im)_2$ frameworks, we performed PXRD and SEM investigations of the transformation with various synthesis temperatures or time which represent the kinetic investigations of $Zn(Im)_2$ formation.

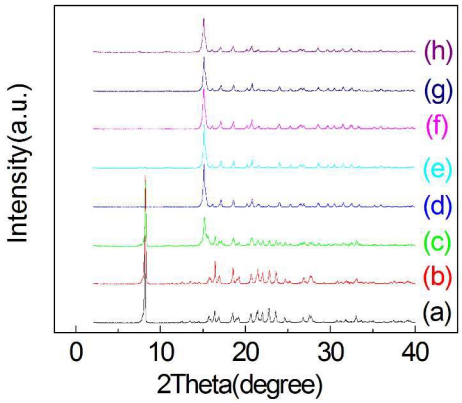

Figure 6. PXRD patterns of (1) after heat treatment in open atmosphere as a function of temperature which was increased at a rate of 5 °C min^{-1}: (b) 100 °C; (c) 125 °C; (d) 150 °C; (e) 200 °C; (f) 250 °C; (g) 300 °C; (h) 350 °C; pattern (a) is as-synthesized (1).

We have observed that (1) can transform to zni (2) in open atmosphere at several temperature (in the range of 150–400 °C) for 24 h. To clarify the structural change in each case, PXRD was used to follow this transformation as a function of temperature. The temperature was increased at a rate of 5 °C min^{-1} in open atmosphere. As shown in Figure 6, the temperature-dependent PXRD studies for (1) heated at 100 °C remain unchanged, indicating that the structural integrity of the framework is maintained. When heated to 125 °C, a mixture of zni (2) and (1) was obtained, indicative of the beginning of a structural transformation. Increasing the temperature to 150 °C results in the complete formation of zni (2) as illustrated by the absence of (1) in the PXRD pattern, indicative of fast structural change and transformation. We kept the reaction ongoing for 250 °C and subsequently for 350 °C, but no further change from the zni (2) was observed. From these observations it is clear that during the period of 100 to 150 °C the (1) starts transforming to the zni (2) in open atmosphere.

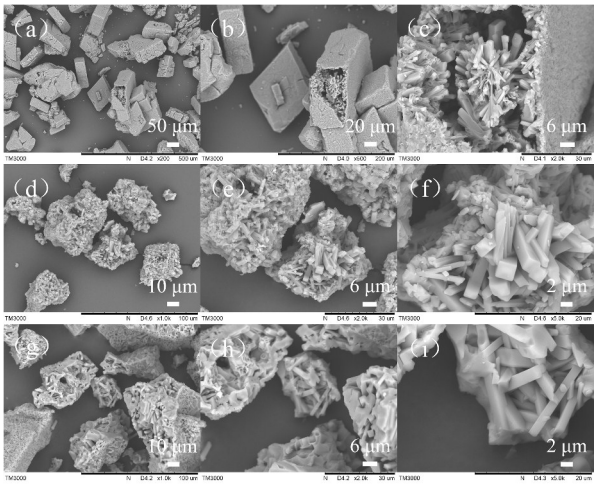

Figure 7. Different magnification SEM images of (1) after heat treatment in open atmosphere as a function of temperature which was increased at a rate of 5 °C min^{-1}: (a, b, c) 125 °C; (d, e, f) 150 °C; (g, h, i) 350 °C.

In addition, SEM images (Figure 7 and Figure S9) show the morphological change of the (1) block-like crystals through phase transformation in open atmosphere. These images indicate that (1) have block-like morphology when the temperature reached 100 °C (Figure S8a), but after that the block-like crystal start broken. After being heated to 125 °C, this was observed in SEM images which show besides the large number of block-like crystal, some broken polycrystalline aggregates which can be assigned to zni (2) (Figure 7a, b, c). From the magnified part of large broken polycrystalline aggregates in Figure 7c, the clusters in the interior of broken crystals are seen to be composed of numerous densely packed rod-like crystals in a disordered array. Increasing the temperature to 150 °C results in the complete transformation from block-like crystal to polycrystalline aggregates (Figure 7d). In addition, After being heated to 200 and 350 °C, polycrystalline aggregates is also observed (Figure 7g, h, i). From the magnified parts of large individual polycrystalline aggregates shown in Figure S9, it can be seen that the polycrystalline aggregates were composed of numerous tightly packed rod-like crystals in a random arrangement.

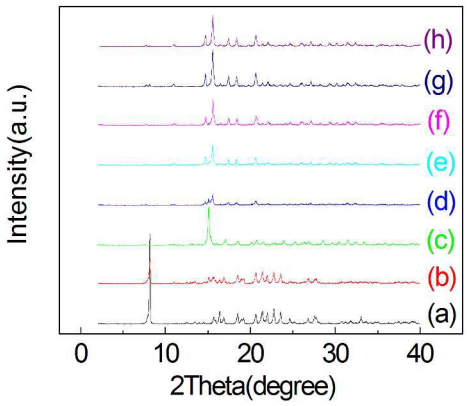

Figure 8. PXRD patterns of (1) after heat treatment in a closed vessel at 150 °C (heated to the reaction temperatures at a rate of 5 °C min^{-1}) as a function of reaction time, the reaction times were (b) 0 h; (c) 0.5 h; (d) 1.5 h; (e) 3 h; (f) 6 h; (g) 12 h; (h) 24 h; pattern (a) is as-synthesized (1).

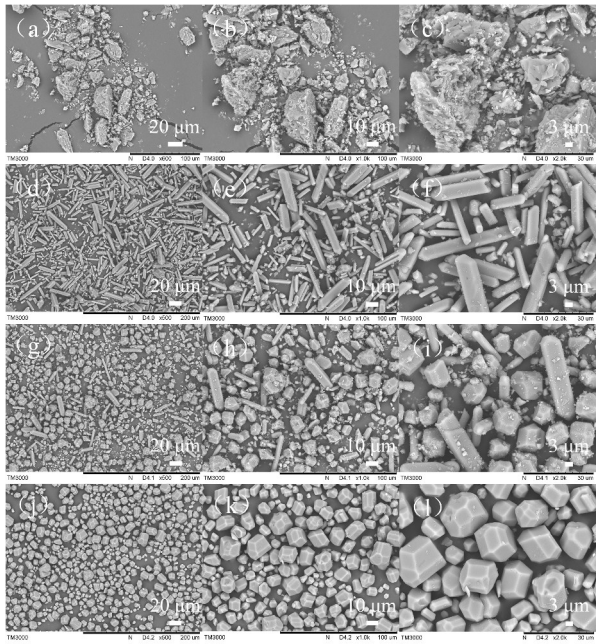

Figure 9. Different magnification SEM images of (1) after heat treatment in a closed vessel at 150 °C (heated to the reaction temperatures at a rate of 5 °C min^{-1}) as a function of reaction time, the reaction times were (a, b, c) 0 h; (d, e, f) 0.5 h; (g, h, i) 1.5 h; (j, k, l) 24 h.

We have observed that (1) can transform to coi (3) in a closed vessel at 150 °C and 180 °C for 24 h, respectively. For this particular study, PXRD was used to follow this transformation in a closed vessel at 150 °C as a function of reaction time (Figure 8). In fact, when the sample was heated to 150 °C at a rate of 5 °C min^{-1}, the PXRD pattern of the sample decreased peak intensity, indicative of the beginning of a structural transformation.

Cite this: DOI: 10.1039/coxx00000x

www.rsc.org/xxxxxx

ARTICLE TYPE

Surprisingly, within the first half an hour, (1) firstly converts into zni. We continued monitoring the phase transformation and at 1.5 h, the characteristic PXRD peaks of zni start disappearing and the relative peak intensity of the coi (3) increases. After 12 h of reaction, the diffraction peaks of zni lose in the PXRD pattern of the reaction product, indicating complete transformation of the formed zni into coi (3). With prolonging the reaction period, the crystallinity of the coi (3) obtained does not show obvious difference.

The typical SEM images of the morphology for coi (3) obtained in the process of the phase transformation are exhibited in Figure 9 and S10. When the temperature reached 150 °C (0 h), these images indicate that the block-like crystal start broken (Figure 9a, b, c). Surprisingly, within the first half an hour, (1) quickly converts into zni, showing its long prismatic crystals morphology (Figure 9d, e, f). Polyhedral crystallites mixed with long prismatic crystals can be observed in the SEM image (Figure 9g, h, i) of the product obtained in the reactant after 1.5 h of the reaction, showing the transformation process from zni to coi (3). After the reaction for 12 h, the long prismatic single crystals disappear (Figure S10f), indicating complete transformation of the formed zni into coi (3). Figure 9k shows a perfect polyhedral crystal of coi (3) with size of 10-20 μm.

Although it is difficult to fully understand the mechanism of phase transition, (especially involving dimensionality changes and structural reorganization), we were able to tentatively propose a possible model on the basis of our results. The transformation process outlined below is only a possible clue to what could happen during the conversion of (1) into 3D $Zn(Im)_2$, upon heating.

The composition of (1) was determined by analysis as $[Zn(Im)(HIm)_2(OAc)]$. Compared to zni (2)-$[Zn(Im)_2]$. (1) contains additional HIm and OAc species in the framework. Thus, the phase transformation in open atmosphere from 1 to zni (2) may proceed with the release of, one coordinating HIm ligands and the noncoordinated OAc anion. The other HIm undergoes deprotonation, becoming a bidentate Im linker bridging two Zn centres. It seems that the structural transformation involves Zn-N coordination bond cleavage and formation. Here the participation of HIm in deprotonation and bonding makes the dimensionality cross-over in the structure. The entire transformation is facile and takes place simultaneously. The kinetic experiments confirmed the rapid phase transformation without formation of an intermediate phase. In contrast, in the formation process of coi (3) in a closed vessel, phase transformation from (1) to zni and from zni to coi (3) was observed, and zni was formed in a short period of the initial reaction stage. We have observed that (1) can transform to coi (3) in a closed vessel at 150 °C and 180 °C for 24 h, respectively. While at high temperature (greater than 200 °C), zni was the main product (Figure S7, left) due to the carbonization and decomposition of released units. Thus, the role of released HOAc and HIm units are also crucial in a closed vessel since they likely play the key roles of structure directing agents in coi (3) synthesis. coi (3) transforms into zni when heated in air at a heating rate of 5 °C min^{-1} to 375 °C with the loss of HOAc and HIm from the framework (Figure S11).

Conclusions

The solvent free reaction of $Zn(OAc)_2$ with an imidazole ligand resulted in a 1D chain structure with a formula, $[Zn(Im)(HIm)_2(OAc)]$. The results suggest that (1) likely evolves from an unidentified phase. Using this 1D chain precursor as a single source of Zn and imidazolate ligand, two $Zn(Im)_2$ frameworks were successfully prepared with known topologies (zni and coi). More importantly, zni (2) and coi (3) were prepared by thermal-mediated transformation when heated in an open and in a closed system, respectively. In the formation of zni (2), the kinetic experiments confirmed the rapid phase transformation without formation of an intermediate phase. In contrast, in the formation process of coi (3), phase transformation from (1) to zni and subsequently from zni to coi (3) was observed. Thus, in a closed system, the released HOAc and HIm were occluded into the framework coi, which seem to paly a structure-directing effect on the formation of coi. Therefore, the syntheses described here is a single precursor approach. The present work represents the first example of the transformation of 1D coordination polymers into 3D ZIF framework. We believe that the single precursor concept or 1D–3D transformation can be easily extended to the synthesis of other ZIF materials.

This work was financially supported by the National Natural Science Funds (Grant No. 51172153, 21306126 and 21136007), the Natural Science Foundation of Shanxi Province (2013021008-1). Y. H. thanks the Natural Science and Engineering Research Council of Canada for a Discovery Grant. We also thank the Centre for Advanced Materials and Biomaterials Research at Western University for a small grant for international collaboration.

Notes and references

[a] *Research Institute of Special Chemicals, Taiyuan University of Technology Taiyuan, 030024, Shanxi, P.R.China. Fax: +86 351 611178; Tel: +86 351 6010550; E-mail: dongjinxiangwork@hotmail.com*

[b] *Department of Chemistry, The University of Western Ontario, London, Ontario, N6A 5B7 (Canada); E-mail: yhuang@uwo.ca*

† Electronic Supplementary Information (ESI) available: [The detailed experimental characterization including PXRD, TG-DSC, N_2 sorption, and FT-IR are described in detail in the Supporting Information]. See DOI: 10.1039/b000000x/

1 (a) A. Phan, C. J. Doonan, F. J. Uribe-Romo, C. B. Knobler, Michael O'Keeffeand O. M. Yaghi, *Acc. Chem. Res.*, 2010, **43**, 58; (b) J. P. Zhang, Y. B. Zhang, J. B. Lin and X. M. Chen, *Chem. Rev.*, 2012, **112**, 1001.

2 (a) Y. Q. Tian, C. X. Cai, X. M. Ren, C. Y. Duan, Y. Xu, S. Gao, and X. Z. You, *Chem. Eur. J.*, 2003, **9**, 5673; (b) Y. Q. Tian, Y. M.

Zhao, Z. X. Chen, G. N. Zhang, L. H. Weng and D. Y. Zhao, *Chem. Eur. J.*, 2007, **13**, 4146.
3 (a) X. C. Huang, Y.Y. Lin, J. P. Zhang and X. M. Chen, *Angew. Chem. Int. Ed.*, 2006, **45**, 1557; (b) J. B. Lin, R. B. Lin, X. N. Cheng, J. P. Zhang and X. M. Chen, *Chem. Commun.*, 2011, **47**, 9185.
4 (a) K. S. Park, Z. Ni, A. P. Côté, J. Y. Choi, R. D. Huang, F. J. Uribe-Romo, H. K. Chae, M. O'Keeffe and O. M. Yaghi, *Proc. Natl. Acad. Sci. USA*, 2006, **103**, 10186; (b) R. Banerjee, A. Phan, B. Wang, C. Knobler, H. Furukawa, M. O'Keeffe and O. M. Yaghi, *Science*, 2008, **319**, 939.
5 (a) T. Wu, X. H. Bu, R. Liu, Z. E. Lin, J. Zhang and P. Y. Feng, *Chem. Eur. J.*, 2008, **14**, 7771; (b) T. Wu, X. H. Bu, J. Zhang and P. Y. Feng, *Chem. Mater.*, 2008, **20**, 7377.
6 (a) Y. L. Liu, V. C. Kravtsov, R. Larsen and M. Eddaoudi, *Chem. Commun.*, 2006, **42**, 1488.
7 B. L. Chen, Z. X. Yang, Y. Q. Zhu and Y. D. Xia, *J. Mater. Chem. A*, 2014, **2**, 16811.
8 Y. C. Pan, D. Heryadi, F. Zhou, L. Zhao, G. Lestari, H. Sub and Z. P. Lai, *Cryst. Eng. Comm.*, 2011, **13**, 6937.
9 H. Cho, J. Kim, S. Kim, W. Ahn, *Microporous and Mesoporous Materials,* 2013, **169**, 180.
10 (a) J. Cravillon, R. Nayuk, S. Springer, A. Feldhoff, K. Huber, and M. Wiebcke, *Chem. Mater.*, 2011, **23**, 2130; (b) J. Cravillon, C. A. Schröder, K. Huber, A. Rothkirch, J. Caro and M. Wiebcke, *Cryst. Eng. Comm.*, 2012, **14**, 492.
11 H. Bux, F. Y. Liang, Y. S. Li, J. Cravillon, M. Wiebcke and J. Caro, *J. Am. Chem. Soc.*, 2009, **131**, 16000.
12 G. A. V. Martins, P. J. Byrne, P. Allan, S. J. Teat, A. M. Z. Slawin, Y. Li, R. E. Morris, *Dalton Trans.,* 2010, **39**, 1758.
13 P. J. Beldon, L. Fábián, R. S. Stein, A. Thirumurugan, A. K. Cheetham, and T. Friščić, *Angew. Chem. Int. Ed.*, 2010, **49**, 9640
14 B. Seoane, J. M. Zamaro, C. Tellez, J. Coronas, *Cryst. Eng. Comm.,* 2012, **14**, 3103.
15 Q. Shi, Z. F. Chen, Z. W. Song, J. P. Li, J. X. Dong, *Angew. Chem. Int. Ed.*, 2011, **50**, 672.
16 (a) J. Cravillon, S. Münzer, Lohmeier, S. J. Feldhoff, A. Feldhoff, K. Huber and M. Wiebcke, *Chem. Mater.*, 2009, **21**, 1410; (b) Y. C. Pan, Y. Y. Liu, G. F. Zeng, L. Zhao and Z. P. Lai, *Chem. Commun.*, 2011, **47**, 2071.
17 M. J. Cliffe, C. Mottillo, R. S. Stein, D. Bučar and T. Friščić, *Chem. Sci.*, 2012, **3**, 2495.
18 O. Karagiaridi, M. B. Lalonde, W. Bury, A. A. Sarjeant, O. K. Farha, and J. T. Hupp, *J. Am. Chem. Soc.*, 2012, **134**, 18790.
19 J. Y. Li, Y. Song, J. H. Yu, P. Chen, and R. R. Xu, *Microporous Mesoporous Mater.*, 2007, **98**, 47.
20 Y. C. Ou, D. S. Zhi, W. T. Liu, Z. P. Ni, and M. L. Tong, *Chem. Eur. J.*, 2012, **18**, 7357.
21 (a) E. C. Spencer, R. J. Angel, N. L. Ross, B. E. Hanson, and J. A. K. Howard, *J. Am. Chem. Soc.*, 2009, **131**, 4022; (b) T. D. Bennett, D. A. Keen, J. C. Tan, E. R. Barney, A. L. Goodwin, and Anthony K. Cheetham, *Angew. Chem. Int. Ed.,* 2011, **50**, 3067; (c) C. A. Schröder, I. A. Baburin, L. Wullen, M. Wiebcke, and S. Leoni, *CrystEngComm*, 2013, **15**, 4036; (d) K. Müller-Buschbaum and F. Schönfeld, *Z. Anorg. Allg. Chem.*, 2011, **637**, 955.
22 (a) B. P. Biswal, T. Panda and R. Banerjee, *Chem. Commun.*, 2012, **48**, 11868; (b) M. E. Schweinefuß, S. Springer, I. A. Baburin, T. Hikov, K. Huber, S. Leoni, and M. Wiebcke, *Dalton Trans.*, 2014, **43**, 3528; (c) Z. X. Low, J. F. Yao, Q. Liu, M. He, Z. Y. Wang, A. K Suresh, J. Bellare, H. T. Wang, *Cryst. Growth Des.*, 2014, **14**, 6589.
23 S. C. Junggeburth, L. Diehl, S. Werner, V. Duppel, W. Sigle and B. V. Lotsch, *J. Am. Chem. Soc.*, 2013, **135**, 6157.
24 R. Lehnert, F. Z. Seel, *Z. Anorg. Allg. Chem.* 1980, **464**, 187.
25 M. Sturm, F. Bromdl, D. Engel, W. Hoppe, *ActaCrystallogr. Sect. B* 1975, **31**, 2369.

A single precursor approach for ZIFs synthesis: Transformation of a new 1D [Zn(Im)(HIm)$_2$(OAc)] structure to 3D Zn(Im)$_2$ frameworks

Qi Shi,[a] Fei Wang,[a] Xiaozhen Kang,[a] Jun Xu,[b] Yining Huang,*[b] Jinping Li[a] and Jinxiang Dong*[a]

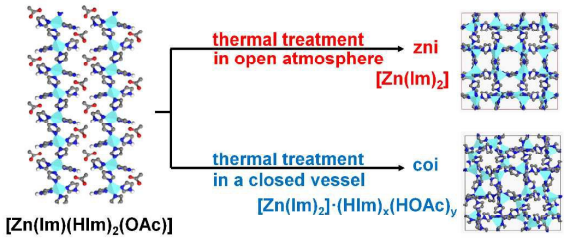

We successfully use 1-dimensional (1D) chain structure [Zn(Im)(HIm)$_2$(OAc)] (Im =imidazolate, HIm = imidazole, OAc=carboxylate) as a single precursor/source of metal and ligand to directly prepare 3-dimensional (3D) [Zn(Im)$_2$] frameworks.